REPORT DOCUMENTATION PAGE

Form Approved
OMB No. 0704-0188

Public reporting burden for this collection of information is estimated to average 1 hour per response, including the time for reviewing instructions, searching existing data sources, gathering and maintaining the data needed, and completing and reviewing this collection of information. Send comments regarding this burden estimate or any other aspect of this collection of information, including suggestions for reducing this burden to Department of Defense, Washington Headquarters Services, Directorate for Information Operations and Reports (0704-0188), 1215 Jefferson Davis Highway, Suite 1204, Arlington, VA 22202-4302. Respondents should be aware that notwithstanding any other provision of law, no person shall be subject to any penalty for failing to comply with a collection of information if it does not display a currently valid OMB control number. **PLEASE DO NOT RETURN YOUR FORM TO THE ABOVE ADDRESS.**

1. REPORT DATE *(DD-MM-YYYY)*
27-03-2006

REPRINT

4. TITLE AND SUBTITLE
Near-Relativistic Electron c/v Onset Plots

5a. CONTRACT NUMBER

5b. GRANT NUMBER

5c. PROGRAM ELEMENT NUMBER
61102F

6. AUTHOR(S)
Kahler, S., and B.R. Ragot*

5d. PROJECT NUMBER
2311

5e. TASK NUMBER
RD

5f. WORK UNIT NUMBER
A1

7. PERFORMING ORGANIZATION NAME(S) AND ADDRESS(ES)
Air Force Research Laboratory/VSBXS
29 Randolph Road
Hanscom AFB MA 01731-3010

8. PERFORMING ORGANIZATION REPORT NUMBER
AFRL-VS-HA-TR-2007-1049

9. SPONSORING / MONITORING AGENCY NAME(S) AND ADDRESS(ES)

10. SPONSOR/MONITOR'S ACRONYM(S)
AFRL/VSBXS

11. SPONSOR/MONITOR'S REPORT NUMBER(S)

12. DISTRIBUTION / AVAILABILITY STATEMENT
Approved for Public Release; Distribution Unlimited.

*Helio Reearch, Nashua, NH

13. SUPPLEMENTARY NOTES
REPRINTED FROM: The Astrophysical Journal, Vol 646, pp 634-641, Jul 20, 2006.

14. ABSTRACT

It is often assumed that the first arriving electrons of a near-relativistic ($E > 30$ keV) electron event are injected at the Sun impulsively and simultaneously at all observed energies and propagate scatter-free to 1 AU. In that case, a plot of the onset times T_0 versus c/v for various electron speeds v should yield the solar injection time T_{inj} and the propagation distance D. In some electron events $D \sim 1.2$ AU, but the inferred injection times are characteristically delayed by ~10 minutes after the start of metric/decametric type III radio bursts believed to be signatures of electron injection. The delays may indicate electron injections not directly associated with the type III bursts, but the delays could also result from gradual or energy-dependent injections or from significant coronal/interplanetary electron scattering, even for well-beamed events. These effects could invalidate the c/v plot analyses. We use *Wind* 3D Plasma and Energetic Particle (3DP) electron data to make c/v onset plots for 80 near-relativistic solar electron events to test for the consistency of the inferred values of D, which are found to be broadly distributed between 0.15 and 2.7 AU. In most cases $D < 1$ AU, an unphysical result partially due to instrumental effects in the high-energy 3DP detector, but also clearly inconsistent with the assumptions of impulsive and energy-independent injection onsets and scatter-free propagation of the electrons. We also discuss how previous results from c/v plot analyses have yielded contradictory and/or challenging injection results for the near-relativistic electrons as well as for gradual and impulsive solar energetic ion events.

15. SUBJECT TERMS
Solar energetic proton events Space weather Interplanetary magnetic field

16. SECURITY CLASSIFICATION OF:			17. LIMITATION OF ABSTRACT	18. NUMBER OF PAGES	19a. NAME OF RESPONSIBLE PERSON
a. REPORT		c. THIS PAGE			S. W. Kahler
UNCLAS	UNCLAS	UNCLAS	SAR	10	19b. TELEPHONE NUMBER *(include area code)* 781-377-9665

THE ASTROPHYSICAL JOURNAL, 646:634–641, 2006 July 20
© 2006. The American Astronomical Society. All rights reserved. Printed in U.S.A.

AFRL-VS-HA-TR-2007-1049

NEAR-RELATIVISTIC ELECTRON *c/v* ONSET PLOTS

S. KAHLER
Air Force Research Laboratory, VSBXS, 29 Randolph Road, Hanscom AFB, MA 01731; stephen.kahler@hanscom.af.mil

AND

B. R. RAGOT
Helio Research, P.O. Box 1414, Nashua, NH 03061
Received 2005 January 31; accepted 2006 March 27

DTIC COPY

20070516024

ABSTRACT

It is often assumed that the first arriving electrons of a near-relativistic ($E > 30$ keV) electron event are injected at the Sun impulsively and simultaneously at all observed energies and propagate scatter-free to 1 AU. In that case, a plot of the onset times T_0 versus c/v for various electron speeds v should yield the solar injection time T_{inj} and the propagation distance D. In some electron events $D \sim 1.2$ AU, but the inferred injection times are characteristically delayed by ~10 minutes after the start of metric/decametric type III radio bursts believed to be signatures of electron injection. The delays may indicate electron injections not directly associated with the type III bursts, but the delays could also result from gradual or energy-dependent injections or from significant coronal/interplanetary electron scattering, even for well-beamed events. These effects could invalidate the c/v plot analyses. We use *Wind* 3D Plasma and Energetic Particle (3DP) electron data to make c/v onset plots for 80 near-relativistic solar electron events to test for the consistency of the inferred values of D, which are found to be broadly distributed between 0.15 and 2.7 AU. In most cases $D < 1$ AU, an unphysical result partially due to instrumental effects in the high-energy 3DP detector, but also clearly inconsistent with the assumptions of impulsive and energy-independent injection onsets and scatter-free propagation of the electrons. We also discuss how previous results from c/v plot analyses have yielded contradictory and/or challenging injection results for the near-relativistic electrons as well as for gradual and impulsive solar energetic ion events.

Subject headings: interplanetary medium — scattering — Sun: particle emission — Sun: radio radiation

1. INTRODUCTION

1.1. *Near-relativistic Electron Injection Times*

It has long been understood that bursts of 2 keV $\lesssim E \lesssim$ 100 keV electrons accelerated near the Sun and observed at 1 AU are nearly always accompanied by solar type III radio bursts (Lin 1985). The velocity dispersion of the electron fluxes produces an instability that results in Langmuir waves that are converted into electromagnetic waves at the local electron plasma frequency and its second harmonic (Melrose 1985). Observations at 1 AU of 326 electron events with $E > 2$ keV during a 15 month period in 1978–1979 by the *International Sun-Earth Explorer 3* (*ISEE-3*) satellite seemed to confirm earlier results from the *Interplanetary Monitoring Platform 6* (*IMP-6*) satellite (Lin et al. 1973) that the type III radio bursts are produced by the 2 to $\gtrsim$10 keV electrons (Lin 1985). Time-intensity observations of higher energy ($E >$ 300 keV) solar electron events from the *Helios* spacecraft showed that those electron injections were also simultaneous with the onsets of the flare hard X-ray and microwave impulsive phases (Kallenrode & Wibberenz 1991; Kunow et al. 1991). In a definitive analysis of 27 electron events with $E > 300$ keV restricted to solar minimum conditions and *Helios* within 0.5 AU of the Sun, Kallenrode & Svestka (1994) found good agreement between onsets of solar type III bursts and inferred electron injections.

The onset times of beamlike (Haggerty & Roelof 2002) or impulsive (Krucker et al. 1999) electron events at 1 AU show velocity dispersion. The better time and energy resolution of the 3D Plasma and Energetic Particle (3DP) experiment (Lin et al. 1995) on the *Wind* spacecraft allowed a determination of solar onset times for $E \gtrsim 30$ keV electrons more precise than the earlier *ISEE-3* observations. Plots of those onset times versus c/v, hereafter called c/v plots, where v is the electron speed, led to the unexpected result that many electron injections at the Sun occurred up to half an hour later than the onsets of the preceding type III bursts. Krucker et al. (1999) found that 12 low-energy ($E \lesssim 25$ keV) electron events were still well associated with type III bursts, but in the majority of the cases (41 out of 58) the injection times of the $E > 25$ keV electrons were delayed beyond the timing onset uncertainties of each electron event and associated coronal and/or interplanetary type III burst. In at least two cases both type III–related $E \lesssim 25$ keV electrons and delayed $E > 25$ keV electrons were found.

The existence of delayed solar electron events was then confirmed by Haggerty & Roelof (2001, 2002) using observations of 79 beamlike 38 keV $< E <$ 315 keV electron events with the Electron, Proton, and Alpha Monitor (EPAM) on the *Advanced Composition Explorer* (*ACE*) spacecraft. They inferred their injection times by shifting the onset time of the highest observed EPAM energy channel by 1.2 AU divided by the electron speed for that channel. The electron injections of the 45 EPAM electron events with associated metric type III bursts were characterized by a median electron injection delay of 9.5 minutes. A similar result was found for the electron injection delays relative to the starts of other kinds of flare electromagnetic emission. Haggerty & Roelof (2002) argued that the correlation coefficients of $r \sim 0.5$ between the 38 and 62 keV peak electron intensities and several flare radio and X-ray parameters provided evidence of only a loose relationship between the intensities of electron events and of the accompanying flares. The EPAM study was recently extended by Haggerty et al. (2003) through 2002 March to include 113 electron events; they found a median delay of 13 minutes between the metric

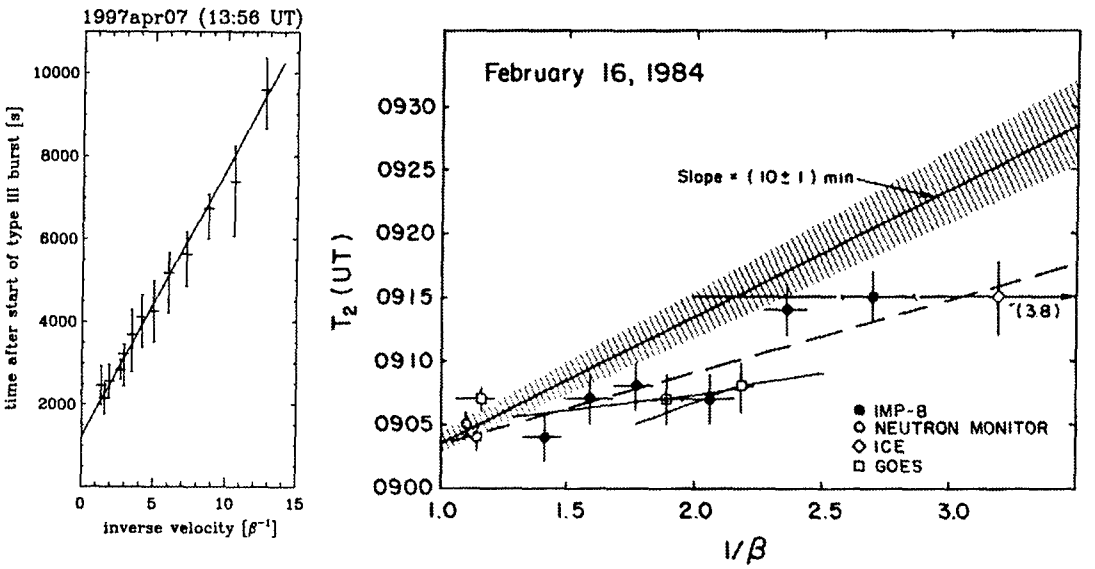

FIG. 1.—*Left:* c/v plot of 3DP electron onsets T_0 for an event on 1997 April 7 (adapted from Krucker et al. 1999). The slope of the line is D/c, and the inferred T_{inj} is given by the intercept of the line with the time axis. The points at $c/v < 3$ are from the 3DP SST, points at $c/v > 3$ are from the EESA. *Right:* c/v plot of the energetic proton T_0 for the SEP event of 1984 February 16, from which Lockwood et al. (1990) deduced that the first ~70 MeV protons ($1/\beta = 2.7$) were injected ~5 minutes before the relativistic protons (neutron monitor). The indicated slope of 10 minutes corresponds to the expected $D = 1.2$ AU. (Adapted from Fig. 11 of Lockwood et al. 1990.)

type III bursts and the electron injection times. The 3DP analysis was extended by Klein et al. (2005) through 2001 May for events with release times during the observations with the Nancay Radioheliograph; they confirmed the frequent occurrence of delayed injections. Several explanations for a physical origin of the delayed injections have been reviewed by Kahler et al. (2005).

The inferred electron injection delays are challenging for several reasons. First, a preceding decametric type III burst was found back at the Sun for nearly every beamlike (Haggerty & Roelof 2002) or impulsive (Krucker et al. 1999) near-relativistic electron event and served as the fiducial to measure the electron injection delay. However, that type III burst is presumed to have no direct physical connection to the subsequent electron injection, except for the few cases with no clear injection delays. A second question is why the delayed electron injections do not produce their own type III bursts (Krucker 2003). The bumps on-tail in the electron energy spectra required for type III emission are presumed to develop (Mann et al. 1999), even with broad power laws in energy extending down to $\lesssim 1$ keV (Lin et al. 1996). In addition, at 1 AU both impulsive electrons and in situ type III bursts are observed simultaneously (Ergun et al. 1998).

Cane (2003) has compared the characteristics of 79 EPAM near-relativistic events with the associated interplanetary type III bursts. She found (1) a correlation between the electron injection delay times and the times required for the associated type III radio bursts to drift to the lowest frequencies, (2) a close correspondence between the electron and local radio emission intensities, and (3) a correlation between the electron injection delay times and the ambient solar wind densities. She concluded that there can be only a single electron population that produces the type III burst and that the electron delay occurs in the interplanetary medium and not at the Sun. Her results await confirmation by other investigators.

Cane's (2003) conclusion challenges the validity of the c/v plots. Krucker et al. (1999) used c/v plots for their analysis but showed plots for only 3 of their 12 electron events extending down to 1 keV in energy. In a comparison with the injection times derived by Krucker from 3DP c/v plots, Haggerty & Roelof (2002) found that their technique of using only a single high-energy EPAM c/v point produced differences with a standard deviation of only 2.5 minutes, which they considered to be in satisfactory agreement with and a validation of their simpler technique. Clearly, the validity of the c/v plots is crucial in deciding between the Cane (2003) interpretation of interplanetary delays and the consensus (e.g., Krucker et al. 1999; Haggerty & Roelof 2002; Klein et al. 2005; Maia & Pick 2004) view of coronal injection delays.

Here, we first discuss in § 1.2 the assumptions and concept of the c/v plots and then in § 2 review how they have been applied to various solar energetic particle (SEP) data sets as the dominant tool for our current understanding of the timing of SEP acceleration and injection. Our goal is to show that use of the c/v plots has produced inconsistent and contradictory results regarding injections of ions and electrons in gradual (§ 2.1) and impulsive (§ 2.2) SEP events (Reames 1999). In § 3 we examine statistically the derived travel distances D of selected 3DP near-relativistic electron events as a test of the validity of the c/v plots. We discuss the results in § 4.

1.2. *c/v Plots*

The basic concept of the c/v plot for charged particles is based on several assumptions. First, the onset of the solar particle injection profile is both impulsive and energy independent. Second, the first particles observed at 1 AU are assumed to propagate scatter free, with pitch-angle cosines $\mu \simeq 1$, along a common travel path of distance D from the coronal injection site to the observer. Under these assumptions,

$$T_0 = T_{inj} + D/v. \quad (1)$$

A plot of T_0 against c/v for the first arriving particles yields a slope D/c and an intercept on the time axis at T_{inj}, the solar injection time (Fig. 1). The path D is taken to be an interplanetary spiral field, dependent on solar wind speed but generally expected to be close to 1.2 AU. In practice, particle beams observed to be highly collimated along the magnetic field are

assumed to satisfy the scatter-free requirement (e.g., Haggerty & Roelof 2002).

The general application of the c/v plots has been to determine the injection times for SEPs of different types or energies relative to each other and relative to solar flare radiative signatures. The derived path length D, which should be in the range 1–2 AU, is taken as a check on the method. However, model validations of the method have been minimal. Kallenrode & Wibberenz (1990) used a numerical focused-transport model of SEPs to study the effects of scattering on SEP event onset times. As perhaps expected, significant onset delays were encountered for particles with sufficiently small scattering mean free paths λ, smooth (i.e., not impulsive) injection profiles, and large radial distances ($\geq$0.5 AU) from the Sun.

In a more comprehensive modeling analysis, Lintunen & Vainio (2004) have used a focused transport model including convection and adiabatic deceleration to test the c/v plot methodology for $3 \leq c/v \leq 60$. For mean free paths $\lambda \sim P^{1/3}$, where P is particle rigidity, the lower rigidity (higher c/v) particles have later arrival times, and the plots yield larger D and delays of $T_{\rm inj}$ from the model values by ~5 minutes. Lintunen & Vainio (2004) note that increasing λ for the low-P particles and decreasing λ for all particles near the Sun can lead to appropriate inferred values of D, but significant (tens of minutes) delays in $T_{\rm inj}$. Finite injection durations of several hours, mimicking shocks, yielded slightly increased values of D and delays of $T_{\rm inj}$ by 5–20 minutes. It is important to note that ~5–80 minute delays of $T_{\rm inj}$ were found in all their models (their Table 2 for 0.13–57 MeV protons) except for cases of an onset occurring on the declining profile of a previous event. Similar numerical transport modeling was carried out by Saiz et al. (2005) for $1 \leq c/v \leq 15$ and different assumptions about injection profiles, interplanetary scattering, and detection thresholds. Their model c/v plots nearly always aligned close to straight lines but also produced errors in injection times, although smaller than those of the lower particle energies modeled by Lintunen & Vainio (2004).

2. APPLICATIONS OF c/v PLOTS TO SEPs

2.1. *Gradual SEP Events*

The c/v plots were used extensively by H. Debrunner and colleagues to investigate solar injections for a series of high-energy SEP events. Based on strong observed anisotropies and large values of λ inferred from an approximation for pitch-angle scattering by Bieber et al. (1986), Debrunner et al. (1988) examined the injection times for protons of 20 MeV $< E <$ 1.3 GeV in the 1984 February 16 ground level event (GLE). Their c/v plot did not yield a straight line but rather suggested that the 50 MeV $< E <$ 500 MeV protons were injected ~4 minutes earlier than the GeV protons. A similar ~5 minute delay of GeV proton injection was found by Lockwood et al. (1990; see Fig. 1) and Debrunner et al. (1990) in analyses of two other GLE events, and Debrunner et al. (1997) found evidence of an ~2 minute delay of a second GLE component in the 1990 May 24 SEP event.

The c/v plots were used by Dalla et al. (2003) to compare $T_{\rm inj}$ for nine SEP events with $E <$ 130 MeV observed both at *Ulysses* and at 1 AU. They found the inferred SEP injections of events at *Ulysses* to be delayed by 100–350 minutes from those found at 1 AU for the same SEP events. Although the delays were organized by the latitudinal displacements of *Ulysses* magnetic footpoints from the associated flare sites, the delays appeared to be too long to be explained by the times for coronal mass ejection (CME) shocks to propagate to higher latitudes. Further, there were no cases of *Ulysses* SEP injections preceding the 1 AU injections.

EPAM and 3DP near-relativistic electron events have been compared via c/v plots with accompanying gradual SEP events to determine their relative inferred injection times. Krucker & Lin (2000) examined 26 such events from the 3DP instrument on *Wind*. They found two classes of 30 keV $< E <$ 6 MeV proton events. Protons of class 1 traveled about 1.2 AU but were injected 0.5–2 hr after the electron injections; protons of class 2 traveled ~2 AU but were injected simultaneously with the electrons. Since early pitch-angle distributions of the protons and electrons in both classes of events were well collimated with the magnetic fields, there was no obvious difference between the two classes of SEP events during their rise phases. For the class 2 protons Krucker & Lin (2000) suggested an energy-dependent injection, thereby implicitly rejecting the validity of the c/v plots for those events.

Mewaldt et al. (2003) compared onsets of 6–88 MeV nucleon^{-1} ions with those of the EPAM 38–315 keV near-relativistic electrons. For the six SEP events with low He^3/He^4 values, presumed to be gradual SEP events, ion injection delays of several tens of minutes relative to the electron injections were found. Their result was consistent with the $E >$ 4 MeV proton injection delays of ~10–40 minutes found for various gradual SEP events observed in the inner heliosphere on *Helios* (Neustock et al. 1985; Bieber et al. 1980; Wibberenz et al. 1989; Kunow et al. 1991). Those ion delays are also characteristic of the class 1 but not the class 2 SEP events at lower energies (Krucker & Lin 2000) discussed above.

Tylka et al. (2003) found from c/v plots of three GLEs that the injection times of all ions from ~2 MeV nucleon^{-1} through ~2 GeV nucleon^{-1} matched those of the near-relativistic electrons and that the injections were delayed by $\geq$5 minutes from the flare impulsive phases. Their result disagrees with the Mewaldt et al. (2003) and earlier *Helios* results regarding the injection delays between the electrons and the ions, and it contradicts the Debrunner et al. (1990) and Lockwood et al. (1990) results of an injection delay in the GeV protons relative to that of the $E <$ 500 MeV protons. The Tylka et al. (2003) result may also be inconsistent with recent work by Huttunen-Heikinmaa et al. (2005), who compared inferred injections of 14–51 MeV nucleon^{-1} protons and helium nuclei for 25 gradual SEP events. They found simultaneous injections for 8 events, but in the remaining 17 events the helium injections were delayed from the proton injections by a median time of 30 minutes.

To summarize, the earlier *Helios* observations at solar distances of 0.3–1.0 AU gave us a simple picture of gradual SEP ion-injection onsets delayed by ~10–40 minutes from those of the near-relativistic electrons. The electron injections coincided with the onsets of the type III radio bursts and the flare impulsive X-ray phases. However, the various c/v plots of ions from more recent SEP gradual events, all at greater solar distances, have shown the various inconsistencies detailed above. In some cases the ion injection onsets coincide with those of the electrons; in others they are delayed. In both situations the generally inferred electron injection delays from the type III bursts contradict the *Helios* results. We suggest that the problem lies in the c/v plots.

2.2. *Impulsive SEP Events*

Impulsive SEP events are characterized by impulsive solar injections, enhanced heavy-element abundances, and high He^3/He^4 ratios (Reames 1999). Early work with particle observations from the *ISEE-3* spacecraft enabled Reames et al. (1985) and Reames & Lin (1985) to associate the impulsive SEP events with both interplanetary energetic (~20 keV) electron events and type III radio bursts. Proton injections of four impulsive $E >$ 4 MeV SEP events

observed on *Helios* at 0.3 AU were found to be simultaneous within 1–2 minutes with injections of $E > 300$ keV electrons and with the onsets of the flare electromagnetic radiation (Kallenrode & Wibberenz 1991). Mason et al. (1989) found good model transport fits to three "scatter-free" impulsive $\sim$1 MeV nucleon^{-1} SEP events, assuming injections at type III burst onsets. Their fits showed that the ion injections had nearly step-function rises and full widths of $\lesssim$1 hr. Kilometric type III burst observations were used by Reames & Stone (1986) to determine the interplanetary trajectories and solar source regions of the strongest He^3-rich events. Their study was done without benefit of energetic electron observations, but each He^3-rich event was found to be associated with a kilometric type III burst. More recently, small CMEs have been found with some impulsive SEP events such as 2000 May 1 (Kahler et al. 2001), but coronal ejecta can be accommodated in a model of impulsive electron and ion injection marked by simultaneous and cospatial type III bursts (Reames 2002). Introducing an average pitch angle into their c/v plots, Klein & Posner (2005) found that the injections of six small 8–25 MeV proton events, including that of 2000 May 1, coincided with decametric-to-hectometric type III bursts. Thus, the established paradigm for impulsive SEP events has been that metric and kilometric type III bursts are the signatures of simultaneous and impulsive injection of both energetic electrons and ions.

Ion and near-relativistic electron observations from the *ACE* spacecraft can serve to test this basic paradigm. Mewaldt et al. (2003) used the c/v plots to determine 6–88 MeV nucleon^{-1} heavy ion injection times and compare them with 38–315 keV electron injection times. For the 5 He^3-rich SEP events of their sample, the ion and electron injections appeared to be nearly simultaneous. Their result was confirmed for two of their five events (2000 May 1 and 2001 April 14) for a larger range of SEP energies by Tylka et al. (2003), who also found those injections to be delayed from the decametric type III bursts.

Ho et al. (2003) used c/v plots to compare the injection times of nine impulsive He^3-rich low-energy (180 keV nucleon^{-1} $< E <$ 10 MeV nucleon^{-1}) ion events with those of the associated near-relativistic electron events. For five of the nine events, they found ion injections delayed from the electron injections by 70–180 minutes, contrary to the simultaneous injections found at higher energies by Kallenrode & Wibberenz (1991) and Mewaldt et al. (2003). A statistical edge technique applied to the ion c/v plots and a 2 σ point prior to intensity maximum to define ion onset times may have biased the Ho et al. (2003) results toward the later ion injections, but in three of the four events with no significant ion injection delays, the electron injection times *preceded* the closest type III burst times by $\gtrsim$0.5 hr. Most of their events were therefore inconsistent with the paradigm that both the impulsive ions and electrons are injected during the type III bursts. Thus, except for the Ho et al. (2003) results, the c/v plots have yielded simultaneous electron and ion injections in impulsive SEP events. However, results of the plots clearly differ from the paradigm that impulsive ion and electron injections are simultaneous with the type III bursts.

3. DATA ANALYSIS

3.1. *Selection of the Near-relativistic Electron Events*

We selected near-relativistic electron events based on two event lists. The first list consists of beamed events observed in the EPAM instrument, given in Table 2 of Haggerty & Roelof (2002) and extended through the end of 2002 (D. Haggerty 2003, private communication). The event selection criteria and a brief description of the instrument are given in Haggerty & Roelof (2002). Each of the two EPAM instruments measures electrons in the $\sim$40 to $\sim$315 keV range in four channels. From their list we selected for analysis only those events observed in the third (103–175 keV) or fourth (175–315 keV) energy channels.

The second event list is the impulsive electron events observed with the 3DP solid-state telescope (SST) previously given at the instrument Web site. The SST measures electrons in the $\sim$25 to $\sim$500 keV energy range in seven channels. The event selection criteria and a brief description of the 3DP instrument and data reduction are given in Ergun et al. (1998) and in Krucker et al. (1999). At the time of data selection that list consisted of two periods, 1994 November 15 to 2001 June 22 and 2002 February 1 to 2002 October 21. From the qualitative assessments of the event data we selected only the SST "mediocre" and "good" events for the analysis. Only the lowest five energy channels ($\sim$30 to $\sim$230 keV) of the SST were used in the analysis.

For a separate study we also required that 40–800 MHz radiospectrographic observations from the Tremsdorf station of the Astrophysical Institute of Potsdam be available from about 1 hr before the inferred electron injection time through the injection time. The Tremsdorf observations are normally made from about 07:00 to 15:00 UT. We selected 80 3DP electron events, of which 34 are also EPAM beamed events. For 24 of the 80 3DP events, the electron enhancements could be adequately observed in the 2 to 27 keV range of the 3DP electron electrostatic analyzer (EESA) to extend the onset analysis to that lower range.

3.2. *Event Onset Times T_0*

For all electron events we determined the onset times for each 3DP energy channel showing a distinct flux increase. Because they must be determined in the presence of a background counting rate, electron onset times are always subject to uncertainty. Krucker et al. (1999) determined a standard deviation σ of the background counting rate, subtracted the background rate from the total counting rate, and then let the time of the 4 σ point define the latest possible onset time. The first preceding time step with a positive flux was taken as the onset time. Those times were consistent with onset times determined by eye. Examples of 3DP counting rate profiles were given by Krucker et al. (1999) and by Ergun et al. (1998).

For each of their EPAM electron events, Haggerty & Roelof (2002) determined by eye onset times in the highest EPAM channel showing a clear flux increase. They then assumed that $D =$ 1.2 AU to derive their solar injection times, which matched very closely ($\sigma = 2.5$ minutes) the injection times from the 3DP instrument using the techniques of Krucker et al. (1999) from the 3DP instrument. In their analysis of EPAM electron events, Maia & Pick (2004) used the 4 σ criterion and the average slope of the counting rate at that point to determine the electron onsets. Their method agreed ($\sigma \leq 2$ minutes) with the values determined by eye by Haggerty & Roelof (2002).

We use the event onset times T_0 to derive D from the c/v plots to test the validity of those plots, so those onset times are obviously important for the analysis. The 3DP backgrounds are generally not steady and often show nondispersive variations on various timescales that can compromise attempts to calculate a preevent background. We determined the 3DP SST and EESA T_0 times by eye, which, compared with the statistical onset determinations, has the advantage of using the background and rise-phase profile information on both short ($\sim$minutes) and long ($\sim$tens of minutes) timescales. Since 34 of our 80 events were also observed in EPAM, we compared our T_0 times with those of the same EPAM events for similar energy channels. The median

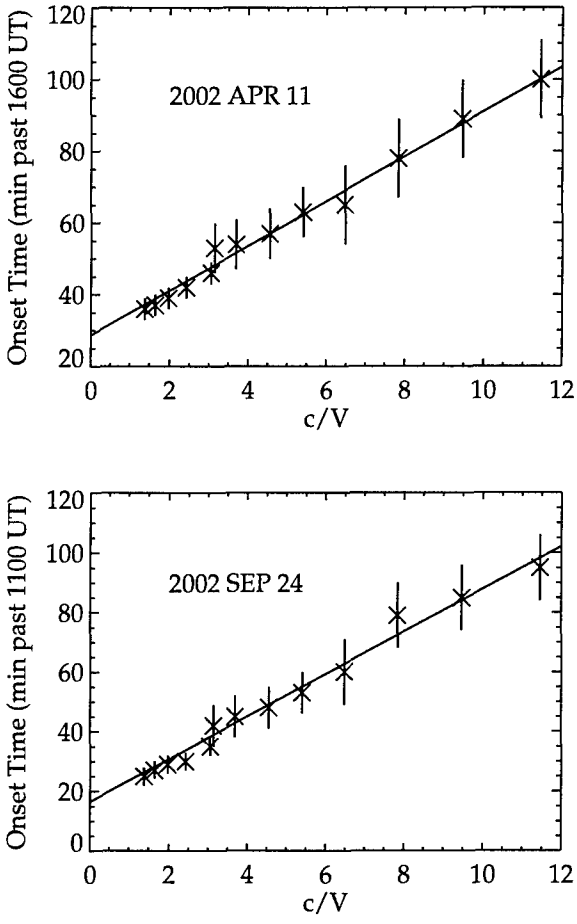

FIG. 2.—Two examples of good fits to the *c/v* plots. *Top:* Event of 2002 April 11 with $D = 0.75 \pm 0.03$ AU. *Bottom:* Event of 2002 September 24 with $D = 0.86 \pm 0.04$ AU.

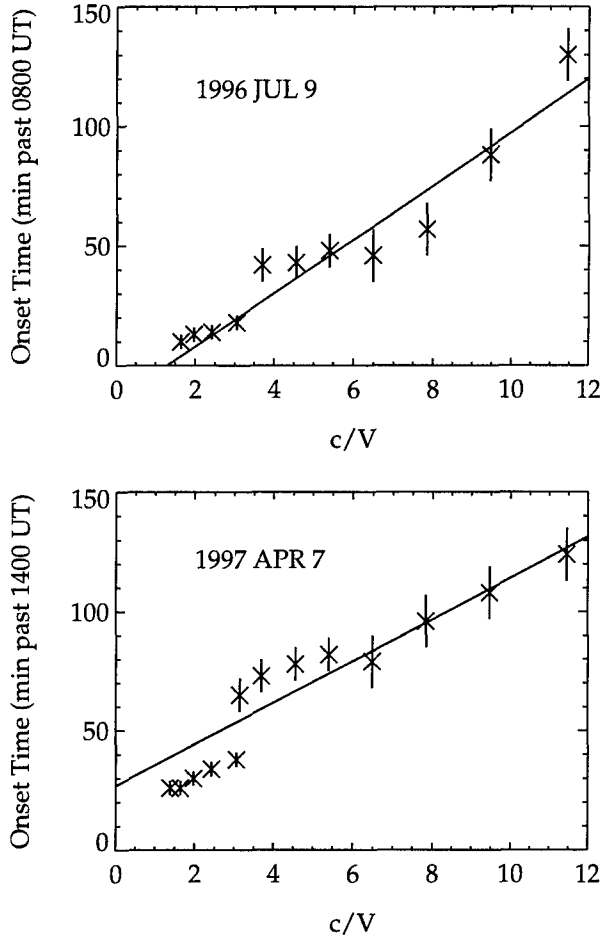

FIG. 3.—Two examples of poor fits to the *c/v* plots. *Top:* Event of 1996 July 9 with $D = 0.75 \pm 0.03$ AU. *Bottom:* Event of 1997 April 7 with $D = 1.05 \pm 0.10$ AU. This is the same event as shown in our Fig. 1 from Krucker et al. (1999).

difference in onsets is 1 minute (3DP times are earlier) and only 7 of the 34 common events have onset time differences exceeding 3 minutes. This indicates good agreement between our 3DP T_0 times and those of Haggerty & Roelof (2002) for EPAM.

3.3. *c/v Plots for Near-relativistic Electron Events*

We have done three sets of *c/v* plots for the 3DP near-relativistic electron events, (1) the 80 SST plots, (2) 23 separate EESA plots, and (3) 24 combined SST and EESA plots. For all events we assumed T_0 uncertainties of 3, 7, and 11 minutes for the five SST energy channels (30–230 keV), the EESA top channels (9–27 keV), and the EESA intermediate channels (2–6 keV), respectively. In Figure 2 we show two example events with relatively good fits and in Figure 3, two with poor fits. The least-squares best fits of the slopes for D were derived. Our concern here is not the inferred T_{inj}, but rather whether the inferred values of D are consistent with those expected for a Parker spiral interplanetary magnetic field (IMF).

The inferred values of D from the 80 SST plots are shown in Figure 4, plotted as functions of the simultaneous values of measured solar wind speeds. The points can be compared against the minimum Parker spiral IMF travel distances (*solid line*) for the corresponding solar wind speeds. Values of D range from 0.15 to 2.7 AU; the distribution median is 0.88 ± 0.09 AU, inconsistent with a realistic D for a solar source. The D exceeds the minimum travel distance for only 16 of the 80 events. Similar results are obtained when we plot the 23 EESA (a two-point plot is omitted) and the 24 combined SST and EESA event D values (Fig. 5) against the solar wind speeds. Those median values of D are 0.95 ± 0.07 AU for the separate EESA events and 0.99 ± 0.06 AU for the combined events.

3.4. *Tests for Validity of T_0 and D*

We have done several tests to look for any dependence of T_0 or D on event characteristics observed in the SST. We first obtained

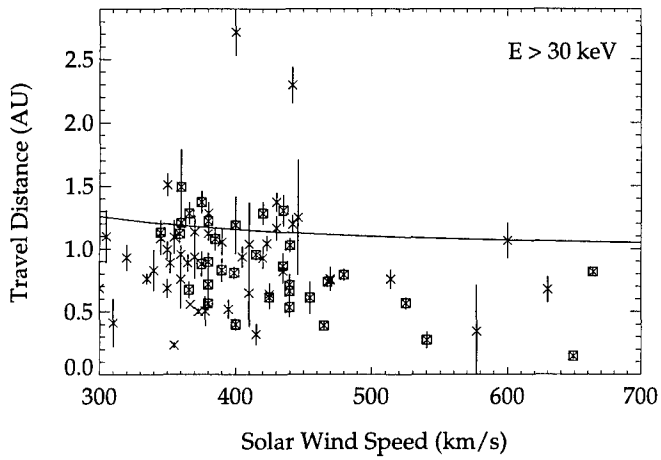

FIG. 4.—Travel distance D as a function of the associated solar wind speed for the onsets of the 80 3DP SST electron events of the study. Squares indicate the beamed EPAM events. The solid line shows corresponding Parker spiral path lengths.

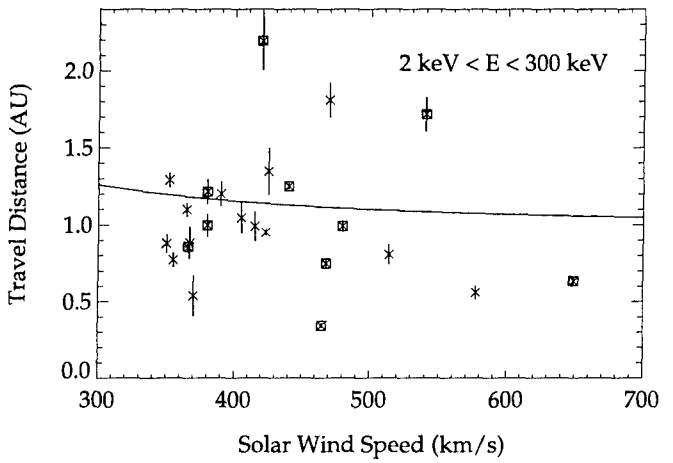

FIG. 5.—Travel distance D as a function of solar wind speed for the 24 combined 3DP low-energy EESA and high-energy SST events. Squares indicate the beamed EPAM events. The solid line shows corresponding Parker spiral path lengths. As with the SST events of Fig. 4, most deduced travel distances D are less than the required minimum distance, and hence are inconsistent with the assumptions of the *c/v* plots.

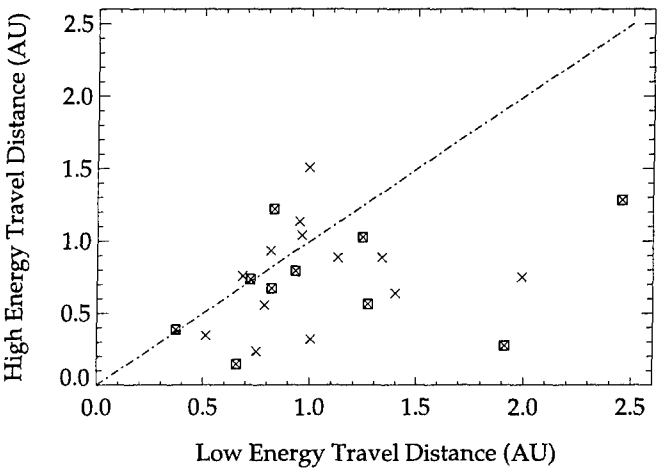

FIG. 7.—D for the SST high-energy (30–230 keV) vs. the EESA low-energy (2–27 keV) components of the 23 3DP electron events. Squares indicate the beamed EPAM events. Equal values for the two components would fall on the diagonal line.

the time intervals ΔT between the T_0 for the 30 and 135 keV energy channels for each of the 80 SST events. In their SEP propagation model, Lintunen & Vainio (2004) found a trend of increasing ΔT (hence increasing D) with smaller peak SEP intensities for their assumed background counting rates. Their preevent background acted to delay onsets of low-energy channels more than those of the high-energy channels. We compared the 80 event ΔT and D values with the corresponding 82 keV peak-to-background ratios and found weak inverse correlations for both, indicating that the more intense electron events are statistically associated with slightly smaller D. Thus, small peak-to-background ratios are not responsible for the cases of $D < 1$ AU.

A dependence could also arise if some electrons in a particular energy range lose only some of their energy in the detector and are registered in lower energy channels (Haggerty & Roelof 2003), resulting in apparently earlier T_0 in those channels. That effect would result in artificially smaller differences of T_0 among the channels and a smaller D for the event. That effect might be more likely for harder electron energy spectra. For a second test we compared both ΔT and D with event power-law spectral exponents obtained for the peak fluxes of the events. Peak energy spectra may not be good indicators of the spectra near event onsets, but we found slightly larger ΔT and D for harder spectra, contrary to what might be expected from this detector effect.

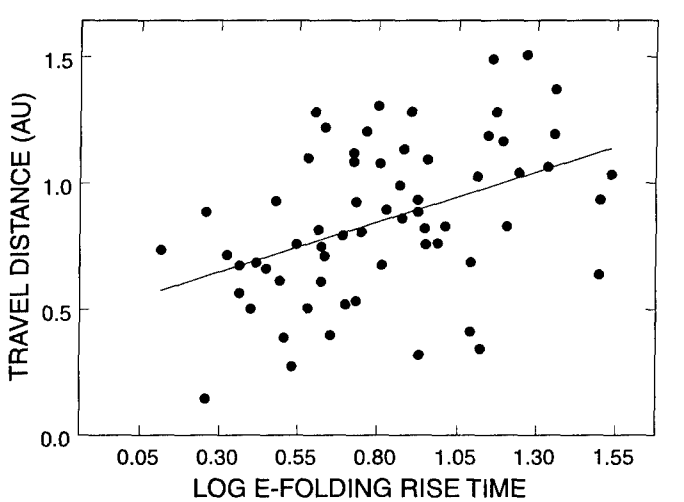

FIG. 6.—Travel distances D for 64 SST high-energy (30–230 keV) electron events vs. log values of the e-folding rise times T_r obtained at event onsets. The line shows the least-squares best fit. The correlation is indicative of cross-channel instrumental effects that produce early T_0 in lower energy channels and smaller D.

There are, however, three indications that the D derived from the SST *c/v* plots (Fig. 4) are partially due to instrumental effects. First, we compared the event T_0 for the 27 keV channel of the EESA detector and for the ~30 keV channel of the SST, which should differ by only ~1–4 minutes, depending on the actual energy bands of the detector channels and on the electron energy spectrum. The event median difference in T_0 is about 6 minutes, suggesting some inconsistency in either the T_0 times or the assumed channel energies. The effect on the resulting *c/v* plots can be judged from Figures 2 and 3, particularly the 1997 April 7 event of Figure 3, for which the 27 minute difference is the worst of all the events.

Second, we did a test similar to that of Huttunen-Heikinmaa et al. (2005), who found $D < 1.2$ AU for 10 of their 25 14–51 MeV SEP events observed with the *Solar and Heliospheric Observatory* (*SOHO*) ERNE instrument and suggested that any cross-channel effects on T_0 should be worse, i.e., produce smaller D, for events with faster rise times at event onsets. Rise times of the ~15 MeV proton intensities of their SEP events correlated ($r = 0.62$) with the D derived from *c/v* plots, indicating some cross-channel effects. For our events we determined the intensity e-folding rise time T_r at the beginning of each event for the 82 keV SST channel. In 16 cases the electron intensity did not reach a factor of e above background, so no value was obtained. Figure 6 shows the correlation ($r = 0.53$, significant at >99%) between D and the log values of T_r, indicating that D is biased by instrumental effects on the SST T_0 and the *c/v* plots derived from them. Third, we compare in Figure 7 the D values of the high-energy SST electrons with those of the 23 low-energy EESA electron events. The systematically larger EESA D values are consistent with artificially small values for the SST D, although effects of an energy-dependent propagation cannot be ruled out.

It is clear that instrumental effects are playing a role in the unphysical values of D obtained from the *c/v* plots. However, values of D cover a large range for the 80 $E > 30$ keV electron events (Figs. 4 and 6), and it is not obvious that cross-channel contamination can explain the entire range. Most of the D values in Figures 4 and 6 lie below the minimum calculated values for D

along the Parker IMF. Even if the values of ΔT and D determined for the SST were artificially small, we have also found the same result with the 24 combined EESA and SST events (Fig. 5) and with the EESA-only events (Fig. 7). In fact, for 16 of the 23 EESA events, the inferred D is less than the minimum calculated D. In addition, we find that neither the combined EESA and SST nor the EESA-only values of D correlate with the log values of the e-folding rise times, contrary to that of the SST values shown in Figure 6, or with event intensities, measured by the 82 keV peak-to-background ratios. Our conclusion is that the derived D values are smaller than the minimum spiral IMF travel distances for a large fraction of the 80 electron event onsets of this study and that the result cannot be due entirely to instrumental effects. The results in those cases call into question the c/v technique for determining T_{inj} for the electrons.

4. DISCUSSION

Fundamental to all studies of solar energetic particle populations observed remotely from the Sun are the time and location of acceleration and injection. For those observations the c/v plots, based on the velocity dispersion of the first arriving particles, may be the only tool for deducing the time and/or source of the injection. We have seen in § 2 that c/v plots have been widely used by many authors to determine injections in different events, but those studies have yielded inconsistent results involving the injection profiles of not only the near-relativistic electron events, but also the gradual (§ 2.1) and impulsive (§ 2.2) ion SEP events. In this work we have put the c/v plots of solar near-relativistic electron events to a test of their consistency with minimal travel distances D and found that in most cases they do not pass that test. This implies that one or more of the assumptions on which the c/v plots are based must be invalid.

An intrinsic limitation to the use of c/v plots is that the SEP onsets are always observed in a particle detector, as they rise above the background counting rates of the detector channel. The investigator is confronted with the problem of determining the profile of the SEP onset as it would appear in the absence of that background, which generally has its own temporal variations and may also be coupled to the SEP signals of other channels of the detector. We briefly summarized in § 3.2 the techniques used by other investigators who have analyzed electron onsets in the EPAM and 3DP detectors. However reasonable those techniques may appear, the actual form of that earliest onset remains unknowable and represents an intrinsic limitation to the c/v plots. In this work we too had to assume that the determined electron onset times were good approximations to "actual" electron onset times at 1 AU.

Even a good straight-line fit and reasonable ($\sim$1.1–2 AU) inferred D for a c/v plot is not a sufficient condition (Saiz et al. 2005) for use of the plot. Krucker (2003) has pointed out that in their (Krucker & Lin 2000) class 2 SEP events, for which they preferred an energy-dependent proton injection, it is surprising that the onset times at 1 AU are still observed to be inversely proportional to the velocity, yielding good c/v plots. Those class 2 proton event onsets yielded $D \sim 2$ AU, but as mentioned in § 1.2, some scattering models can produce event onsets with reasonable D but significantly delayed T_{inj}, despite an impulsive injection of the particles (Lintunen & Vainio 2004). Thus, even the events of Figures 4 and 5 close to the spiral IMF distances may yield T_{inj} significantly delayed from the actual injection times.

Use of the c/v plots assumes that the solar injection profiles are both energy independent and characterized by rise times sufficiently impulsive to produce well defined detector onsets at 1 AU. Energy independence could be violated when trapping conditions at the Sun allow an earlier escape of higher-energy particles or when acceleration to the higher energies of the injected spectrum occurs on an extended timescale. These energy-dependent injections would obviously undermine use of the c/v plots and were not considered in the Lintunen & Vainio (2004) and Saiz et al. (2005) models. However, those authors did consider injection profiles with extended rise times and found both injection time delays and D to increase with the injection durations.

We have used the calculated spiral IMF distances as our fiducial in Figures 4 and 5, but field-line wandering induced by turbulence is theoretically expected (Ragot 1999, 2006*b*, 2006*c*; Ruffolo et al. 2004) and inferred from some type III burst profiles (Reames & Stone 1986). Field-line lengths in corotating interaction regions may be subspiral (Schwadron & McComas 2005) and hence shorter than the idealized values, but the prevalence of field-line wandering and wobbling will lead to path lengths longer than the ideal spiral values, with even fewer derived values of D shown in Figures 4 and 5 satisfying those minimal lengths.

Scatter-free propagation for the particles of the event onsets is another key assumption for the c/v plots. Recent work has shown that near-relativistic electrons are scattered primarily in gyroresonant interactions with whistler waves and nonresonant wave-particle interactions (Ragot 2005, 2006*a*). The strong increase with energy of the whistler scattering of 10 keV to 1 MeV electrons may explain the low inferred values of D. The extreme dependence of nonresonant interactions on the electron pitch angle would be consistent with a low pitch-angle filtering and possible trapping of the electrons before their arrival. Models including these realistic scattering processes can be tested against electron observations from instruments such as the EPAM and 3DP detectors. The observational aspect of solar particle injection would also greatly benefit from a satellite mission to the inner heliosphere, such as the NASA Living with a Star Sentinels Mission (Lin & Szabo 2005), where SEPs can be observed with minimal scattering, as made clear by the results from the *Helios* mission (Kunow et al. 1991).

S. K. acknowledges the support of a Window on Europe grant from the Air Force Office of Scientific Research and thanks the solar group at the Astrophysikalisches Institut Potsdam, where much of the work was done. S. Krucker provided help with the 3DP software, and D. Haggerty provided the EPAM beamed electron event list. B. R. acknowledges support from NASA grant NNG 04GB15G and thanks the Air Force Research Laboratory at Hanscom Air Force Base for computer resources as a visitor with S. K. The critical comments of the persistent and indomitable referee led to significant improvements in this work.

REFERENCES

Bieber, J. W., Earl, J. A., Green, G., Kunow, H., Müller-Mellin, & Wibberenz, G. 1980, J. Geophys. Res., 85, 2313
Bieber, J. W., Evenson, P. A., & Pomerantz, M. A. 1986, J. Geophys. Res., 91, 8713
Cane, H. V. 2003, ApJ, 598, 1403
Dalla, S., et al. 2003, Ann. Geophys., 21, 1367
Debrunner, H., Flückiger, E., Grädel, H., Lockwood, J. A., & McGuire, R. E. 1988, J. Geophys. Res., 93, 7206
Debrunner, H., Fluckiger, E. O., & Lockwood, J. A. 1990, ApJS, 73, 259
Debrunner, H., et al. 1997, ApJ, 479, 997
Ergun, R. E., et al. 1998, ApJ, 503, 435
Haggerty, D. K., & Roelof, E. C. 2001, in Proc. 27th Int. Cosmic Ray Conf. (Katlenburg-Lindau: Copernicus), 8, 3238
———. 2002, ApJ, 579, 841
———. 2003, Adv. Space Res., 32, 423

Haggerty, D. K., Roelof, E. C., & Simnett, G. M. 2003, Adv. Space Res., 32, 2673
Ho, G. C., Roelof, E. C., Mason, G. M., Lario, D., & Mazur, J. E. 2003, Adv. Space Res., 32, 2679
Huttunen-Heikinmaa, K., Valtonen, E., & Laitinen, T. 2005, A&A, 442, 673
Kahler, S. W., Aurass, H., Mann, G., & Klassen, A. 2005, in IAU Symp. 226, Coronal and Stellar Mass Ejections, ed. K. P. Dere, J. Wang, & Y. Yan (Cambridge: Cambridge Univ. Press), 338
Kahler, S. W., Reames, D. V., & Sheeley, N. R., Jr. 2001, ApJ, 562, 558
Kallenrode, M.-B., & Svestka, Z. 1994, Sol. Phys., 155, 121
Kallenrode, M.-B., & Wibberenz, G. 1990, in Proc. 21st Int. Cosmic Ray Conf. (Adelaide), 5, 229
———. 1991, ApJ, 376, 787
Klein, K.-L., Krucker, S., Trottet, G., & Hoang, S. 2005, A&A, 431, 1047
Klein, K.-L., & Posner, A. 2005, A&A, 438, 1029
Krucker, S. 2003, in Energy Conversion and Particle Acceleration in the Solar Corona, ed. L. Klein (Berlin: Springer), 179
Krucker, S., Larson, D. E., Lin, R. P., & Thompson, B. J. 1999, ApJ, 519, 864
Krucker, S., & Lin, R. P. 2000, ApJ, 542, L61
Kunow, H., Wibberenz, G., Green, G., Müller-Mellin, R., & Kallenrode, M.-B. 1991, in Physics of the Inner Heliosphere II, ed. R. Schwenn & E. Marsch (Berlin: Springer), 243
Lin, R. P. 1985, Sol. Phys., 100, 537
Lin, R. P., Evans, L. G., & Fainberg, J. 1973, Astrophys. Lett., 14, 191
Lin, R. P., & Szabo, A. 2005, in Proc. SPIE 5901, 255
Lin, R. P., et al. 1995, Space Sci. Rev., 71, 125
———. 1996, Geophys. Res. Lett., 23, 1211
Lintunen, J., & Vainio, R. 2004, A&A, 420, 343
Lockwood, J. A., Debrunner, H., & Flückiger, E. O. 1990, J. Geophys. Res., 95, 4187
Maia, D. J. F., & Pick, M. 2004, ApJ, 609, 1082
Mann, G., Jansen, F., MacDowall, R. J., Kaiser, M. L., & Stone, R. G. 1999, A&A, 348, 614
Mason, G. M., Ng, C. K., Klecker, B., & Green, G. 1989, ApJ, 339, 529
Melrose, D. 1985, in Solar Radiophysics, ed. D. J. McLean, & N. R. Labrum (Cambridge: Cambridge Univ. Press), 177
Mewaldt, R. A., et al. 2003, in Proc. 28th Int. Cosmic Ray Conf. (Tokyo), 6, 3313
Neustock, H.-H., Wibberenz, G., & Iwers, B. 1985, in Proc. 19th Int. Cosmic Ray Conf. (La Jolla), 4, 102
Ragot, B. 1999, ApJ, 525, 524
———. 2005, ApJ, 619, 585
———. 2006a, ApJ, 642, 1163
———. 2006b, ApJ, 644, 622
———. 2006c, ApJ, in press
Reames, D. V. 1999, Space Sci. Rev., 90, 413
———. 2002, ApJ, 571, L63
Reames, D. V., & Lin, R. P. 1985, in Proc. 19th Int. Cosmic Ray Conf. (La Jolla), 4, 273
Reames, D. V., & Stone, R. G. 1986, ApJ, 308, 902
Reames, D. V., von Rosenvinge, T. T., & Lin, R. P. 1985, ApJ, 292, 716
Ruffolo, D., Matthaeus, W. H., & Chuychai, P. 2004, ApJ, 614, 420
Saiz, A., Evenson, P., Ruffolo, D., & Bieber, J. W. 2005, ApJ, 626, 1131
Schwadron, N. A., & McComas, D. J. 2005, Geophys. Res. Lett., 32, L03112
Tylka, A. J., et al. 2003, in Proc. 28th Int. Cosmic Ray Conf. (Tokyo), 6, 3305
Wibberenz, G., Kecskemety, K., Kunow, H., Somogyi, A., Iwers, B., Logachev, Yu.I., & Stolpovskii, V. G. 1989, Sol. Phys., 124, 353